Two-Fluid Equilibrium Considerations of $T_e/T_i \gg 1$, Collisionless ST Plasmas Sustained by RF Electron Heating*)

Yueng-Kay Martin PENG[1,2)], Akio ISHIDA[3)], Yuichi TAKASE[2)], Akira EJIRI[2)], Naoto TSUJII[2)], Takashi MAEKAWA[4)], Masaki UCHIDA[4)], Hideki ZUSHI[5)], Kazuaki HANADA[5)] and Makoto HASEGAWA[5)]

[1)]*Oak Ridge National Laboratory, Oak Ridge, TN 37831, U.S.A.*
[2)]*The University of Tokyo, Kashiwa 277-8561, Japan*
[3)]*Nishi-Ku, Niigata 950-2161, Japan*
[4)]*Kyoto University, Kyoto 606-8501, Japan*
[5)]*Kyushu University, Kasuga 816-8580, Japan*

(Received 10 December 2013 / Accepted 21 April 2014)

A solution of two-fluid (electron and ion), axisymmetric equilibrium is presented that approximates solenoid-free plasmas sustained only by RF electron heating that are recently studied in TST-2, LATE, QUEST. These plasmas indicate presence of orbit-confined energetic electrons carrying substantial toroidal current outside the last closed flux surface (LCFS); $T_e/T_i \gg 1$ and low collisionality at modest densities within LCFS; and likely a positive plasma potential relative to the conductive vacuum vessel. A system of nonlinear second-order partial differential and algebraic equations constraining six functionals of poloidal magnetic flux or canonical angular momentum are solved. An example plasma measured in TST-2 is used to guide, by trial and error, the selection of these functionals to find appropriate solutions, while assuming peaked plasma profiles and 60% toroidal current within the LCFS. The numerical equilibrium obtained indicates a substantial ion toroidal flow and electrostatic potential so that the ion ∇p_i, centrifugal, and electrostatic forces of nearly equal magnitudes combine to balance the $J_i \times B$ force, differently from the massless electron fluid that satisfies $\nabla p_e = J_e \times B$. The calculated properties suggest additional measurements needed to refine the choices of the functional forms and improve the two-fluid equilibrium fit to such plasmas.

Keywords: solenoid-free spherical tokamak plasma, axisymmetric equilibrium, electron-ion two-fluid plasma with flow, heated electron and colder ion, electrostatic potential, nonlinear second order partial differential equation and algebraic equation, functional of poloidal flux and canonical angular momentum, finite differencing, successive over relaxation

DOI: 10.1585/pfr.9.3403146

1. Introduction

This paper presents a first example of 2-fluid equilibria [1] that approximates solenoid-free RF-only ST plasmas with $T_e/T_i \gg 1$ observed recently in TST-2 [2, 3], together with a summary of the model and numerical approaches [4]. Such plasmas are similar in nature to those also observed in LATE [5], QUEST [6], and MAST [7]. Calculation of such equilibrium will help understand the electron and ion fluid force balance properties in these plasmas, and provide an equilibrium basis for further studies of particle orbits, plasma stability, transport, current drive, boundary, and the plasma-wall interface.

This paper will address experimental observations of interest; 2-fluid equilibrium model reduced from the first principles; experimental conditions used to constrain choices of otherwise arbitrary input functions; the initial results; and summary and discussion.

2. Experimental Observations and Suggestions

The properties characterizing these plasmas can be described with the help of the MHD equilibrium modeled for an RF-only LATE plasma [5] shown in Fig. 1. It is expected that the LCFS stays far within the boundary of toroidal current density j_ϕ. The plasma region external to the LCFS is populated by orbit-confined energetic electrons (100-500 keV) of very low n_e ($10^{16-17}/m^3$), while the LCFS is populated by plasmas of lower T_i (10 - 100 eV) and T_e (50 - 300 eV) and higher n_e (up to several $10^{18}/m^3$). On QUEST copious keV-level ion or neutral impact sites are evident on tungsten coupons on wall [8], thus a likely positive plasma potential. I_p/P_{RF} in the range of 0.1 - 0.4 A/W are observed. More recently, $I_p/P_{RF} \leq 1$ A/W is observed on MAST [9].

A positive plasma potential would result where the

author's e-mail: takase@k.u-tokyo.ac.jp
*) This article is based on the presentation at the 23rd International Toki Conference (ITC23).

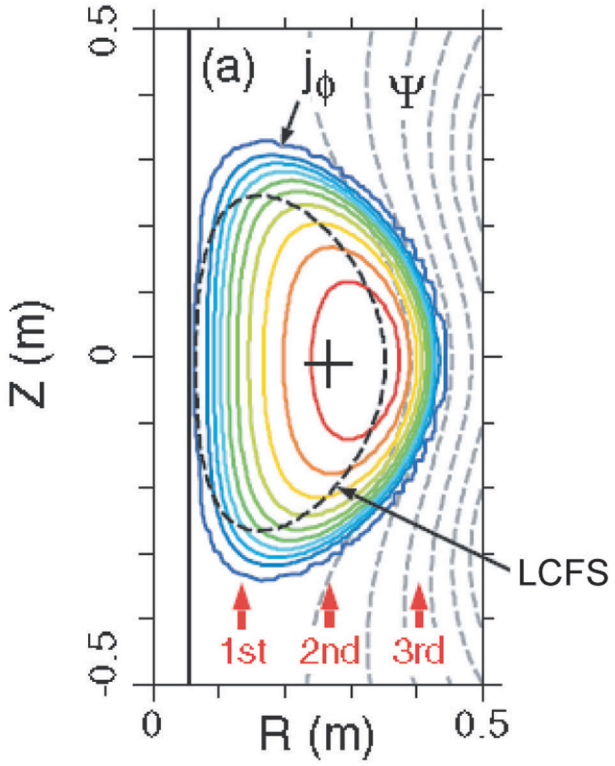

Fig. 1 Equilibrium modeled for a LATE plasma [5]. Reprinted figure with permission from M. Uchida, T. Yoshinaga, H. Tanaka, and T. Maekawa, Phys. Rev. Lett. 104, 065001 (2010). Copyright 2010 by the American Physical Society.

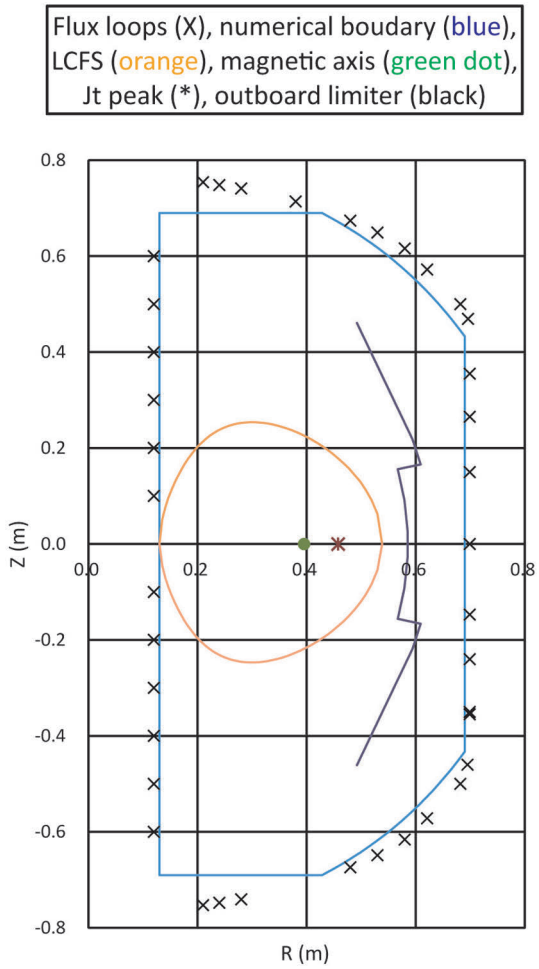

Fig. 2 Boundary conditions used to solve $\psi(R, Z)$ that approximates a TST-2 plasma (#75467@60 ms).

slower loss rate of ions, compared to the fast electrons, leads to an ambipolar potential to accelerate the ions toward the wall. The radial electric field E_r would cause a substantial toroidal ion flow via $E_r \times B_p$. These in turn would cause substantial centrifugal and electrostatic forces of the ion fluid to contend with the ∇p_i and $J_i \times B$ forces. The electron fluid with negligible mass would not encounter this complexity. As a result a two-fluid equilibrium model is required in this first attempt to model such ST plasmas.

3. Two-Fluid Equilibrium Model [1,4]

This model is based on the standard continuity, force balance, and Ampere's law for the electron and ion fluids:

$$\nabla \cdot (n\boldsymbol{u}_\alpha) = 0 \qquad \text{for } \alpha = \text{e and } \alpha = \text{i},$$
$$-(\nabla p_\alpha + m_\alpha n \boldsymbol{u}_\alpha \cdot \nabla \boldsymbol{u}_\alpha) + q_\alpha n(\boldsymbol{E} + \boldsymbol{u}_\alpha \times \boldsymbol{B}) = 0,$$
$$\nabla \times \boldsymbol{B} = \mu_0 en(\boldsymbol{u}_i - \boldsymbol{u}_e),$$

where $n_i = n_e = n$, and $\boldsymbol{u}_\alpha$ is the fluid flow. The importance of the two-fluid regime can be indicated by

$$f_{\text{2F-one}} \equiv \frac{\langle|(en)^{-1}(\nabla p_i + m_i n \boldsymbol{u}_i \cdot \nabla \boldsymbol{u}_i) \times B|\rangle}{\langle|\boldsymbol{E} \times \boldsymbol{B}|\rangle},$$
$$f_{\text{2F-H}\alpha\text{ll}} \equiv \frac{\langle|(en)^{-1}\nabla p_e \times B|\rangle}{\langle|\boldsymbol{E} \times \boldsymbol{B}|\rangle}.$$

Here standard (one-fluid) MHD is adequate when $f_{\text{2F-one}} \ll 1$, and Hall-MHD approximation is adequate when $f_{\text{2F-Hall}} \ll 1$. Otherwise the two-fluid model is required.

The standard equations can be transformed in axisymmetric configuration to two nonlinear 2nd order partial differential equations and six nonlinear algebraic equations containing six functionals of poloidal magnetic flux ψ: T_e, T_i, F_i (ion energy including flow and potential), F_e (electron energy including potential), K (toroidal magnetic flux), and Φ_i (ion poloidal momentum) as functions of ψ and canonical toroidal angular momentum $Y_i(\psi)$.

A finite-differencing method is combined with successive over relaxation (SOR) to solve these equations for a given set of functional forms and numerical boundary conditions. A progressive multi-grid scheme is used to speed numerical convergence.

4. TST-2 Experimental Conditions

A TST-2 hydrogen plasma (#75467@60 ms) is chosen to help find, by trial and error, appropriate functional forms that approach the experimental conditions. This plasma is

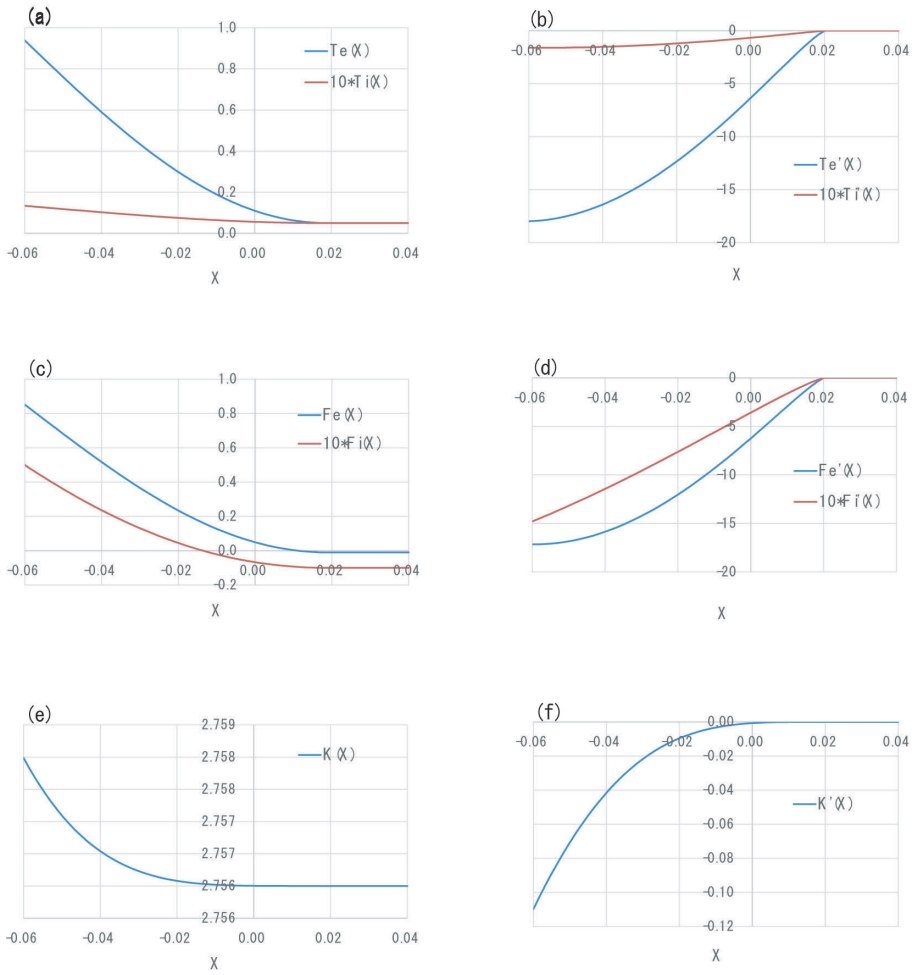

Fig. 3 Functionals chosen for the two-fluid equilibrium calculated: (a) T_e and T_i, (b) T'_e and T'_i, (c) F_e and F_i, (d) F'_e and F'_i, (e) K, and (f) K' vs. $X = \psi/\psi_{ref}$ or Y_i/ψ_{ref}, where $\psi_{ref} = 0.0126$ Wb/rad.

inboard limited and characterized by $B_T = 1.26$ kG, $I_p = 10$ kA, $T_e \sim 300$ eV, $T_i \sim$ 10's eV, and $n_e \sim 8 \times 10^{17}/m^3$. The boundary values to solve ψ(R,Z) are located in Fig. 2 along the solid blue line, which is just inside of the experimental flux loops (×), which are attached to the inside vessel wall. These ψ values are interpolated from an EFIT modeling [10] of the plasma that uses the flux loop data and modeled vessel eddy currents. As a result only plasma current occupies the space within this boundary. The outboard limiter contour that limits the distribution of the fast electrons is also indicated.

It is further assumed that about 60% of the I_p falls within the LCFS, and the plasma profiles are centrally peaked to simplify the functional forms. For the case presented, these functionals are plotted in Figs. 3a-3f.

The ion poloidal momentum Φ_i is also assumed to be zero, limiting the ion current to the toroidal direction. The plasma toroidal current density j_ϕ can be expressed as follows:

$$j_\phi = nR\begin{bmatrix} F'_i(Y_i) + F'_e(\psi) \\ -(T'_i(Y_i) + (T'_e(\psi))\ln n \end{bmatrix} + \frac{1}{R}K'(\psi)K(\psi),$$

and is set to zero at and beyond the outer limiter.

5. Example Two-Fluid Equilibrium Properties

The surface plots for $\psi(R, Z)$, $j_\phi(R, Z)$, $n_e(R, Z)$, $T_e(R, Z)$, and electrostatic potential $V_E(R, Z)$ of the two-fluid equilibrium are shown in Fig. 4. Here the values of ψ, j_ϕ, n_e, T_e, and V_E are normalized by $\psi_{ref} = 0.0126$ Wb/rad, $j_{ref} = 10$ kA/m^2, $n_{ref} = 10^{18}/m^3$, $T_{ref} = 0.78$ keV, $V_{ref} = 0.78$ kV, respectively. The results indicate that the LCFS occupies a relatively small area of the vessel cross section with an elongation of 1.23 (see, Fig. 2). The toroidal current density j_ϕ occupies the space up to the ψ value defined by the outboard limiter and is distributed far beyond the LCFS. The peak of j_ϕ is located at a larger R than the magnetic axis (see, * and • in Fig. 2, respectively). Plasma current within the LCFS is calculated to be 59% of I_p, with an I_z (net vertical current along mid-plane) of about 5% of I_p. The n_e peaks further outboard in R, with a larger fraction of the plasma particles still contained within the LCFS. These centrally peaked profiles are consequences

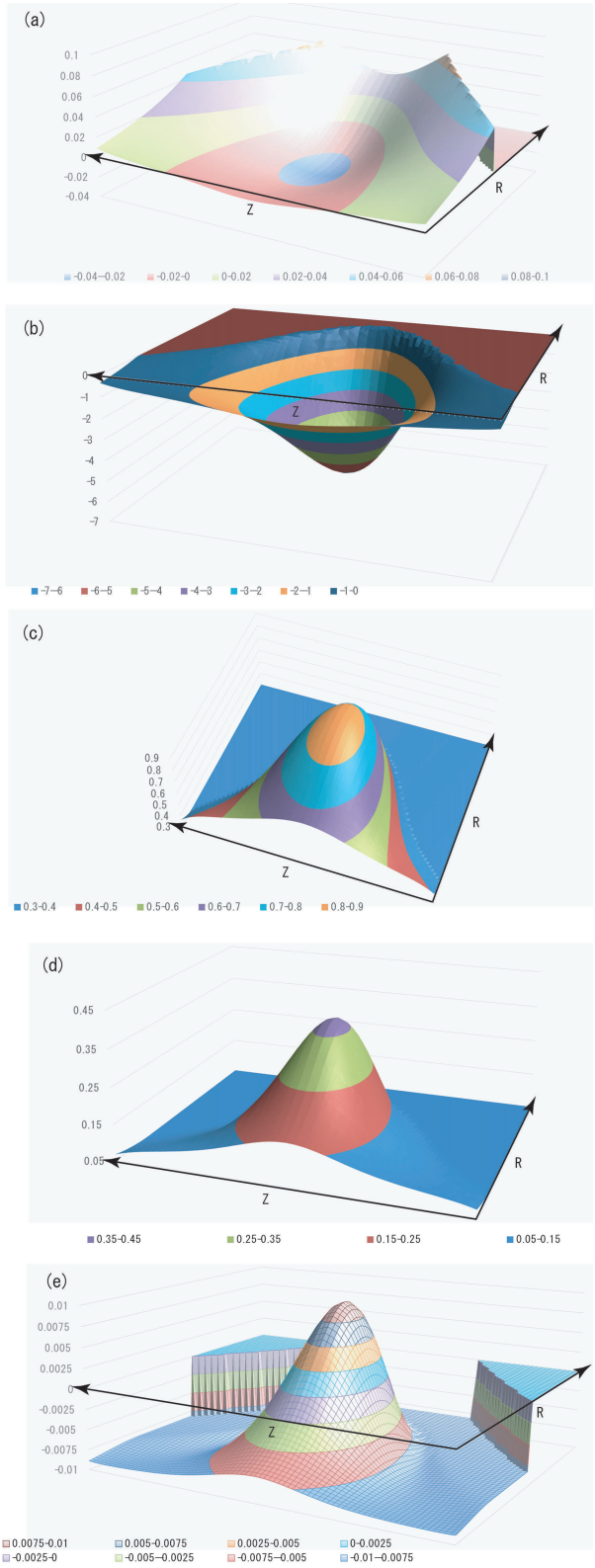

Fig. 4 Surface plots of the calculated two-fluid equilibrium in normalized quantities: (a) $\psi(R, Z)$, (b) $j_\phi(R, Z)$, (c) $n_e(R, Z)$, (d) $T_e(R, Z)$, (e) electrostatic potential $V_E(R, Z)$.

of the assumed functional forms. Finite values of j_ϕ, n_e, and T_e, along the inboard boundary are indicated. These suggest a need to refine the functional forms to adjust the profiles and change these values if necessary. The electrostatic potential V_E is largely confined within the LCFS and peaked at the outboard side of the magnetic axis.

Plasma profiles along the mid-plane are shown in Fig. 5. It is seen that V_E is ~ 14 V positive relative to the boundary value and is larger than the peak T_i ($\sim$10 eV); ion flows in the co-current direction and contributes to increase I_p; plasma pressure peaks at ~ 40 Pa; electron flow velocity $u_{e\phi}$ is much smaller than the electron thermal velocity v_{the} while the ion flow velocity $u_{i\phi}$ can be more than twice v_{thi}; and E_r-shear and shear reversal are substantial in this plasma. These characteristics of the ion fluid are relatively unusual in the field of equilibrium calculations.

Finally the force balance conditions are provided in Fig. 6. It is seen that the electron fluid force balance is close to the one-fluid MHD condition of $\nabla p_e = J_e \times B$, a direct consequence of the assumed massless electrons. The ion fluid force balance is relatively complex. Outboard of the magnetic axis, the ∇p_i, centrifugal, and electrostatic forces of nearly equal magnitudes combine to balance the $J_i \times B$ force. Inboard of the magnetic axis, the centrifugal force switches to the side of $J_i \times B$ force to balance the combination of ∇p_i and electrostatic forces, which are directed toward the machine axis. The plasma is in the two-fluid equilibrium regime.

The values of $f_{2F\text{-one}}$ and $f_{2F\text{-Hall}}$ are found to be $\sim$1 and $\sim$ 10, respectively, indicating that neither conventional MHD nor Hall MHD approximations would be appropriate in modeling this type of plasma.

6. Summary and Discussion

In this paper we reported the first-time calculation of a two-fluid equilibrium in which the electron and ion fluid force balance conditions are different due to strong centrifugal and electrostatic forces acting on the ion fluid. This calculation has been motivated by solenoid-free RF-driven plasmas with $T_e/T_i \gg 1$, observed so far in TST-2, LATE, and QUEST.

The electron and ion fluid continuity equations, force balance equations, and the Faraday law provided the necessary basis for this two-fluid equilibrium model. Six functionals of poloidal magnetic flux ψ within two nonlinear partial differential equations and six nonlinear algebraic equations are solved via finite differencing with successive over relaxation (SOR) and a progressive multi-grid scheme. A TST-2 plasma of this type and boundary conditions were used to guide, by trial and error, the selection of these six functionals of poloidal magnetic flux ψ and the canonical angular momentum $Y_i(\psi)$.

Despite rather simplified functional forms, the calculated results shed new light on the properties of this type of equilibrium that are different from the one-fluid or Hall MHD approximations. Particularly, the presence of large toroidal currents outside the LCFS was obtained with strong plasma potential and ion toroidal flow self-consistently within the model. The result has thus provided

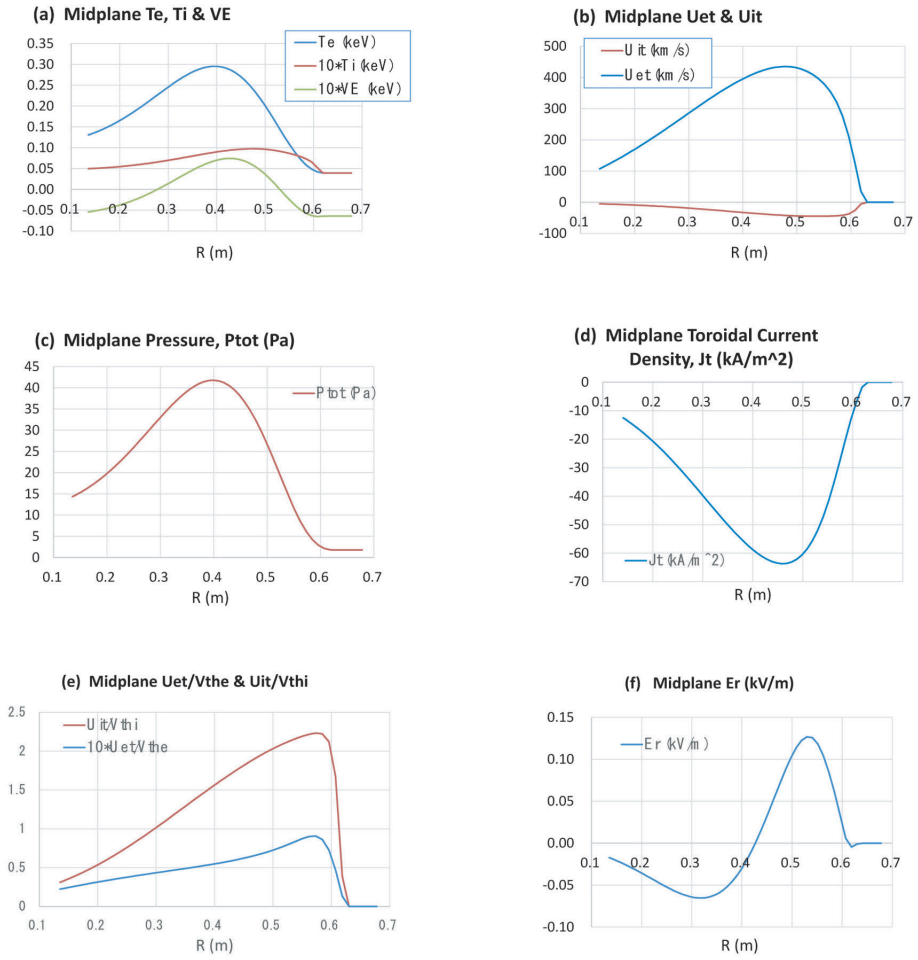

Fig. 5 Plasma profiles along the mid-plane: (a) T_e and T_i in keV and V_E in kV, (b) $u_{i\phi}$ and $u_{e\phi}$ in km/s, (c) plasma pressure in Pa, (d) j_ϕ in kA/m^2, (e) $u_{i\phi}/v_{thi}$ and $u_{e\phi}/v_{the}$, (f) radial electric field E_r in kV/m.

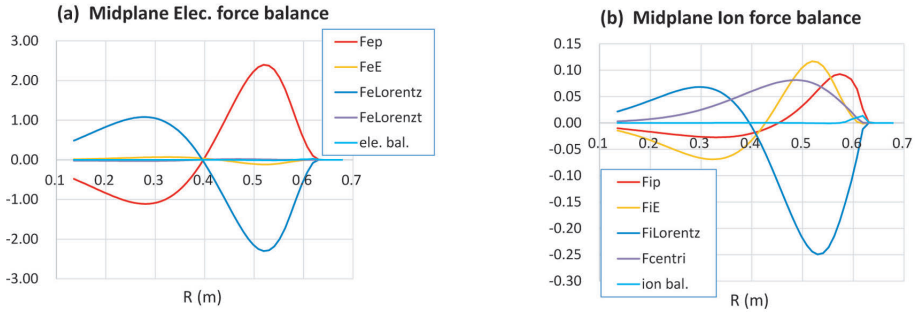

Fig. 6 Plasma force balance conditions in the unit of 0.126 kN/m^3 of (a) the electron fluid ($F_{ep} = -\partial p_e/\partial R$, $F_{eE} = -n_e E_r$, $F_{eLorentz} = J_{e\phi} \times B_z$, $F_{eLorenzt} = -J_{ez} \times B_\phi$), and (b) the ion fluid ($F_{ip} = -\partial p_i/\partial R$, $F_{iE} = n_i E_r$, $F_{iLorentz} = J_i \times B_z$, $F_{centri} = n_i u_{i\phi}^2/R$). "ele. bal." and "ion bal." indicate the deviation from exact force balance.

a magnetic and electrostatic field configuration with which to re-calculate the guiding-center orbit confinement properties of the energetic electrons within the vacuum vessel and the lower temperature ions within the LCFS.

A number of interesting plasma equilibrium features are noted that might have resulted from the selected functional forms rather than the intrinsic properties of this type of equilibrium. The resolution of such uncertainties will require not only additional experimental measurements but also continued improvements in the chosen functional forms. Examples include the magnitude of vertical current along the open field lines, the plasma potential, ion flow, not to mention the separate profiles of the energetic electrons within the vacuum vessel and the thermalized plasmas within the LCFS.

[1] A. Ishida, L.C. Steinhauer and Y.K.M. Peng, Phys. Plasmas **17**, 122507 (2010).
[2] Y. Takase *et al.*, Nucl. Fusion **53**, 063006 (2013).
[3] T. Watatsuki *et al.*, IEEJ Trans. FM **132**, 485 (2012).
[4] A. Ishida and L.C. Steinhauer, Phys. Plasmas **19**, 102512 (2012).
[5] M. Uchida *et al.*, Phys. Rev. Lett. **104**, 065001 (2010).
[6] K. Hanada *et al.*, Plasma Sci. Technol. **13**, 307 (2011).
[7] V. Shevchenko *et al.*, Nucl. Fusion **50**, 022004 (2010).
[8] S.K. Sharma *et al.*, Fusion Eng. Des. **87**, 77 (2012).
[9] F. Shevchenko, T. Bigelow and J. Caughman, private communications.
[10] L.L. Lao *et al.*, Nucl. Fusion **25**, 1611 (1985).